Free Energy Component Analysis: A Study of the Glutamic Acid 165 → Aspartic Acid 165 Mutation in Triosephosphate Isomerase

Valerie Daggett, Frank Brown,† and Peter Kollman*

Contribution from the Department of Pharmaceutical Chemistry, University of California, San Francisco, California 94143. *Received February 4, 1988*

Abstract: We present the results of free energy perturbation calculations on triosephosphate isomerase (TIM) and on a TIM mutant in which the active site Glu 165 is replaced by Asp. It has been experimentally observed that K_M is relatively unaffected by this mutation and that k_{cat} drops roughly 3 orders of magnitude.[1] By selectively changing key electrostatic interactions/hydrogen bonds, we semiquantitatively assessed the role of these interactions in both the binding and turnover of the substrate dihydroxyacetone phosphate (DHAP). Substrate binding was addressed by perturbing residues in the active site and portions of the substrate. We found similar free energy changes for the various perturbations in both the wild-type and the mutant enzyme-substrate noncovalent complexes, suggesting that these interactions contribute equally to substrate binding in the two structures. Wild-type and mutant covalent enzyme-substrate complexes (transition-structure models) were employed in an attempt to elucidate the molecular interactions responsible for the drop in k_{cat} upon mutation. Our results indicate that the drop in catalytic activity may be due, at least in part, to less effective interactions between an electrophilic residue in the active site (Lys 13) and the non-phosphate portion of DHAP in the mutant transition state model. The general approach outlined here, which we refer to as free energy component analysis, should be useful for gaining qualitative mechanistic insight into many binding and reactive processes.

The ability to selectively modify individual amino acids in proteins has been of great use in furthering our understanding of the underlying forces governing enzyme action. The best candidate for studying these interactions, and how they change when mutations are introduced, is an enzyme that is well characterized in mechanistic and energetic terms. Triosephosphate isomerase (TIM) is one such enzyme. Knowles and co-workers have extensively analyzed the TIM-catalyzed reversible isomerization of dihydroacetone phosphate (DHAP) to glyceraldehyde 3-phosphate (GAP).[2] We chose to study this system because of the wealth of kinetic data on both native TIM and a variety of mutants.

The catalytic mechanism of TIM is shown schematically in Figure 1. After substrate binding, the carboxyl group of Glu 165 abstracts the *pro-R* proton from the C1 position of DHAP, resulting in an enzyme-bound enediol, or enediolate. A proton is then delivered to the C2 position of the substrate, yielding GAP. An electrophilic residue is thought to polarize the carbonyl group in the enzyme-substrate complex, thereby facilitating proton abstraction (Figure 1).[3] It has also been suggested that this electrophilic residue stabilizes the developing negative charges on the oxygens at C1 and C2 during formation of the enediol (or enediolate) by providing the substrate with a positive electrostatic environment. On the basis of the X-ray structure by Banner et al.,[4-6] Lys 13 and His 95 appear to be good candidates. On the basis of mutagenesis experiments, Ser 96 also appears to be catalytically important. Knowles and co-workers[7] have characterized a Ser 96 → Pro mutant with interesting properties; proline in this position causes a decrease in the activity of wild-type TIM but increases the activity of the Asp 165 mutant.

TIM has been called a "perfect" enzyme,[2] partly because the rate-determining transition state for the reaction is that for product dissociation and not a chemical step. When Glu 165 is replaced by Asp, by site-directed mutagenesis techniques, the catalytic activity drops roughly 3 orders of magnitude.[1] The Asp 165 mutant employs the same catalytic mechanism as wild-type TIM; however, the process is no longer diffusion controlled.[8] The rate-determining transition state for the Asp mutant is that for formation of the enediol (or enediolate) intermediate, such that the mutant enzyme conforms to the classical Michaelis-Menten scheme. Binding of substrate, enediol/enediolate (as inferred by inhibitor binding), and product is only minimally affected upon mutation.[9]

Our goal was to examine molecular interactions in the active site that might explain the drop in k_{cat} upon replacing Glu 165 with Asp, as well as to examine substrate binding. To this end, we employed the free energy perturbation method, which uses molecular dynamics to evaluate a statistical mechanically derived formulation of free energy.[10] The free energy perturbation method has been shown to be very effective in calculating solvation free energies,[11] binding free energies,[12] and catalytic free energies[13] that are in good agreement with relevant experiments.

To date, the free energy perturbation method has been applied to systems for which the X-ray data are very accurate, thereby allowing a reasonably complete representation of the aqueous environment around the macromolecule-ligand complex. These applications have involved changing the residue of interest in the noncovalent and covalent complexes and comparing the calculated free energies to those inferred from experimental measurements of the differences between k_{cat} and K_M for the wild-type and mutant structures.[13]

The available X-ray crystal structures of chicken muscle TIM and its complexes are only known to low resolution (2.5[4,5] and 6.0 Å,[14] respectively). Thus, our objective was, by necessity,

† Present address: Smith Kline and French Laboratories, King of Prussia, PA 19406.

(1) Straus, D.; Raines, R.; Kawashima, E.; Knowles, J. R.; Gilbert, W. *Proc. Natl. Acad Sci. U.S.A.* **1985**, *82*, 2272.
(2) Knowles, J. R.; Albery, W. J. *Acc. Chem. Res.* **1977**, *10*, 105.
(3) Belasco, J. G.; Knowles, J. R. *Biochemistry* **1980**, *19*, 472.
(4) Banner, D. W.; Bloomer, A. C.; Petsko, G. A.; Phillips, D. C.; Pogson, C. I.; Wilson, I. A. *Nature* **1975**, *255*, 609.
(5) Banner, D. W.; Bloomer, A. C.; Petsko, G. A.; Phillips, D. C.; Wilson, I. A. *Biochem. Biophys. Res. Commun.* **1976**, *72*, 146.
(6) Banner, D. W.; Bloomer, A. C.; Petsko, G. A.; Phillips, D. C.; Pogson, C. I. *Cold Spring Harbor Symp. Quant. Biol.* **1971**, *36*, 151.
(7) Hermes, J. D.; Blacklow, S. C.; Gallo, K. A.; Bauer, A. J.; Knowles, J. R. *UCLA Dupont Symposium. Protein Structure and Design*; Liss: New York, 1987.
(8) Blacklow, S. C.; Raines, R. T.; Lim, W. A.; Zamore, P. D.; Knowles, J. R. *Biochemistry* **1988**, *27*, 1158.
(9) Raines, R. T.; Sutton, E. L.; Straus, D. R.; Gilbert, W.; Knowles, J. R. *Biochemistry* **1986**, *25*, 7142.
(10) Singh, U. C.; Brown, F. K.; Bash, P. A.; Kollman, P. A. *J. Am. Chem. Soc.* **1987**, *109*, 1607.
(11) Bash, P. A.; Singh, U. C.; Langridge, R.; Kollman, P. A. *Science* **1987**, *236*, 564.
(12) Bash, P. A.; Singh, U. C.; Brown, F. K.; Langridge, R.; Kollman, P. A. *Science* **1987**, *235*, 574.
(13) Rao, S. N.; Singh, U. C.; Bash, P. A.; Kollman, P. A. *Nature* **1987**, *328*, 551.

0002-7863/89/1511-8247$01.50/0

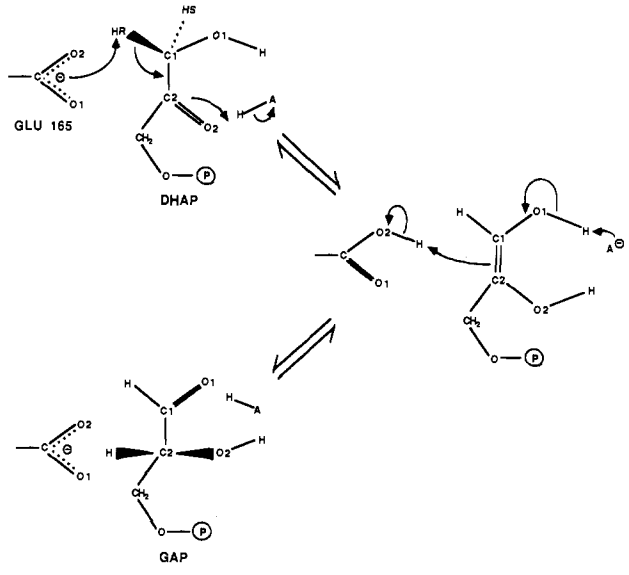

Figure 1. Reaction catalyzed by triosephosphate isomerase (TIM). HA is an electrophilic residue(s)—probably lysine 13 and/or histidine 95—that stabilizes the developing negative charge on the substrate carbonyl oxygen (O2) during formation of the enediol/enediolate intermediate.

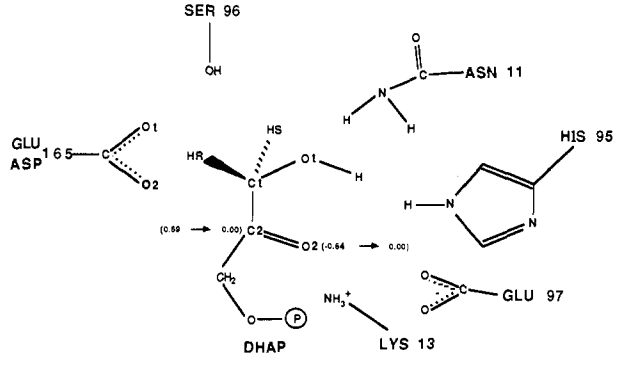

Figure 2. Schematic representation of active site of TIM. Substrate (DHAP) and key active site residues of TIM. The O2 dipole perturbation is depicted. Numbers in parentheses represent initial, unperturbed charges and final, perturbed charges.

qualitative in nature. Compared to earlier studies, we took a slightly different approach, which we refer to as a free energy component analysis. We calculated the free energies for perturbing the charge distributions of various residues in the active site (Asn 11, Lys 13, His 95, Ser 96, Glu 97) and portions of the substrate (O1 and O2 dipoles) in the covalent and noncovalent complexes of both the wild-type and mutant enzymes. Asn 11 and Glu 97 were selected for study in addition to the key catalytic residues (Lys 13, His 95, Ser 96) discussed above because of their proximity to the substrate. Cys 126 is another potential hydrogen-bonding group in the active site, but it was not considered because it is over 7 Å from the catalytically important substrate atoms. (See Figure 2 for a schematic representation of the relative positions of these residues in the active site.) By taking this approach of systematically changing electrostatic interactions in the active site, we hoped to avoid the problems noted above and also arrive at a more detailed interpretation of the roles of those residues that are important in substrate binding and catalysis. This approach is qualitative rather than quantitative in nature but can point out the importance of particular interactions that can be tested experimentally.

By analyzing the free energies for perturbing various groups in the wild-type TIM and DHAP noncovalent complex and the mutant noncovalent complex (Glu 165 replaced by Asp), we examined the interactions important for substrate binding in the two structures. A comparison of the covalent wild-type substrate complex (carboxylate of residue 165 linked to *pro-R* hydrogen of DHAP) and the covalent mutant–substrate complex (which are models of the transition structure for enolization) allowed us to evaluate qualitatively the interactions that stabilize the transition state. These results aided in interpreting the drop in k_{cat} upon mutation. k_{cat} can be decomposed to yield k_{enol}, as the rate constants for individual steps in the conversion of DHAP to GAP have been determined by Knowles and co-workers for the Asp 165 mutant TIM ($k_{enol} = 2.0\ s^{-1}$)[4] and wild-type TIM ($k_{enol} = 2.0 \times 10^3\ s^{-1}$).[2] We compared our results to changes in k_{cat}, but one reaches the same conclusions if the rate constants for enolization are considered.

Methods

Calculation of Free Energy Changes. Except where noted below, calculations were performed with AMBER version 3.0.[15] We calculated Gibbs (G) free energy changes using eq 1, where ΔH is the difference

$$\Delta G = -RT \ln \langle \exp(-\Delta H/RT) \rangle_{ref} \quad (1)$$

in the Hamiltonian between two states, ΔG is the free energy difference between these states, R is the gas constant, T is the absolute temperature, and the symbol $\langle\ \rangle_{ref}$ indicates that an ensemble average is taken with respect to some reference state. (See reference 10 for a more thorough discussion of the method.) In the cases discussed here, H represented the interaction energy of the perturbed group with its surroundings. These interaction energies were calculated at intermediate points along the conversion pathway by use of an empirical force field. Molecular dynamics at 300 K was used to generate the ensemble of structures.

In the applications of this approach published to date, we have reported free energies due only to the intergroup interactions.[10-13] There are many cases where it is advantageous not to include intragroup effects. For example, when one mutates the charges on the oxygen of R–CO–NH–R to zero, there is a very large energy associated with a change in O···H nonbonded interactions. To calculate separately any intergroup effect of the oxygen interacting with its environment, one would need to carry out the mutation of the oxygen for the fragments by itself (which includes only intragroup effects) and in the presence of its environment (which includes both intra- and intergroup effects). This separation is easy to do operationally but involves finding a small difference between large numbers. Instead, one can define CO–NH as the perturbing group, even though the properties of the N–H group do not change, and only consider the intergroup interactions (the intermolecular interactions of this group with its environment). So, when we included particular atoms as part of the system that changes while holding their molecular mechanical parameters constant, the free energy change for the "perturbation" of these atoms was zero. This approach was taken to examine interactions between Lys 13 and specific groups in the active site.

General Formalism for Component Analysis. (A) Perturbation of Substrate Atoms.

Consider the following pathways for binding and catalysis of ligands by an enzyme E and a site-specific mutant E′, where S is the substrate and D denotes a dummy substrate:

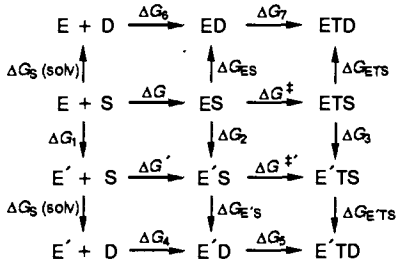

ES corresponds to the enzyme–substrate noncovalent complex and ETS to the transition state for the enzyme-catalyzed reaction. We are interested in the difference in binding free energy, $\Delta\Delta G_{bind} = \Delta G' - \Delta G$, and catalytic free energy, $\Delta\Delta G_{cat} = \Delta G^{\ddagger\prime} - \Delta G^{\ddagger}$, between the enzyme and its site-specific mutant. As noted by Rao et al.[13] in their studies of subtilisin mutants, it is usually easier to calculate ΔG_1, ΔG_2, and ΔG_3 rather than ΔG, $\Delta G'$, $\Delta G^{\ddagger}$, and $\Delta G^{\ddagger\prime}$ and to use the fact that free energy is a state function to determine $\Delta\Delta G_{bind} = \Delta G_2 - \Delta G_1$ and $\Delta\Delta G_{cat} = \Delta G_3 - \Delta G_2$. However, in some cases, such as here for TIM, the direct de-

(14) Phillips, D. C.; Rivers, P. S.; Sternberg, M. J. E.; Thornton, J. M.; Wilson, I. A. *Biochem. Soc. Trans.* **1977**, *5*, 642.

(15) Singh, U. C.; Weiner, P. K.; Caldwell, J.; Kollman, P. A. AMBER 3.0; University of California, San Francisco, 1986.

termination of ΔG_1, ΔG_2, and ΔG_3 is more difficult. Instead, an indirect path can be used to estimate contributions to $\Delta\Delta G_{bind}$ and $\Delta\Delta G_{cat}$. This involves mutating the substrate (S) or transition state (TS) into dummy atoms (D or TD). By using the above thermodynamic cycle, we see that $\Delta\Delta G_{bind} = [\Delta G_{E'S} - \Delta G_S(solv) + \Delta G_4] - [\Delta G_{ES} - \Delta G_S(solv) + \Delta G_6]$ collapses to $\Delta\Delta G_{bind} = \Delta G_{E'S} - \Delta G_{ES}$, assuming that the wild-type and mutant enzyme have the same affinity for dummy substrate (e.g., $\Delta G_4 = \Delta G_6$). Similarly, $\Delta\Delta G_{cat} = \Delta G_{E'TS} - \Delta G_{ETS} - (\Delta G_{E'S} - \Delta G_{ES})$. Thus, the determination of $\Delta\Delta G_{bind}$ and $\Delta\Delta G_{cat}$ involves the mutation of the substrate atoms into dummy atoms both in the noncovalent complex and in a model transition state structure. We also can mutate selected substrate atoms into dummy atoms to estimate the contributions of groups of substrate atoms to binding or catalysis.

In the computational implementation of this approach, we mutated only the electrostatic partial charges of the substrate (S) into those of the dummy molecule (D) to determine particular electrostatic contributions to $\Delta G_{E'S}$, ΔG_{ES}, $\Delta G_{E'TS}$, and ΔG_{ETS}. Therefore, we assumed that the van der Waals contribution to the free energies was equal for ΔG_{ES} and $\Delta G_{E'S}$ and for ΔG_{ETS} and $\Delta G_{E'TS}$. This appears to be a reasonable approximation, because the van der Waals contributions involve "disappearing" the same atoms in each of these cases. Computationally, though, the determination of van der Waals changes involves much more extensive sampling than electrostatic changes. Given our simple model of the enzyme active site (no water inclusion), such a determination would likely be inaccurate and involve large statistical errors. Thus, such an approximation makes sense in this case.

(B) Formalism for Perturbing Enzyme Atoms in Native vs Mutant Enzymes. We also seek a formalism for estimating the contributions of various protein atoms to differential binding and catalysis of an enzyme and its site-specific mutant. We begin with the following thermodynamic cycle:

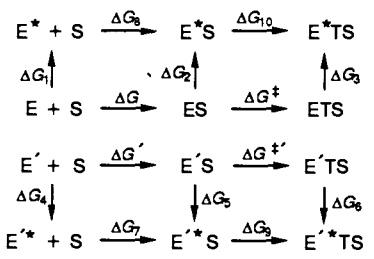

The nomenclature for the scheme above is essentially the same as for the substrate perturbations with the addition of E*, E*S, and E*TS, which correspond to the native enzyme, its complex with substrate, and transition state structure with particular atoms changed to dummy atoms. E'*, E'*S, and E'*TS correspond to the mutant enzyme with the same sets of changes. Here our goal is to calculate

$\Delta\Delta G^*_{bind}$ = contribution to binding from atoms changed to dummies in mutant vs native = $\Delta G' - \Delta G + \Delta G_8 - \Delta G_7$

$\Delta\Delta G^*_{cat}$ = contribution to catalysis from atoms changed to dummies in mutant vs native = $\Delta G^{\ddagger\prime} - \Delta G^{\ddagger} + \Delta G_{10} - \Delta G_9$

and to estimate the experimental $\Delta\Delta G_{bind}$ and $\Delta\Delta G_{cat}$ by the sum of the $\Delta\Delta G^*_{bind}$ and $\Delta\Delta G^*_{cat}$, respectively, for all of the functionally important atoms in the molecule. Interactions between perturbed residues are overcounted when the contributions to $\Delta\Delta G_{bind}$ and $\Delta\Delta G_{cat}$ are summed. This is remedied, though, by subtracting the contribution to the free energy of each combination of perturbed groups from the total.

To proceed further, we made the assumption that we can formally break down the ΔG values into two components: (a) the change in intragroup energies for changed atoms and (b) the interaction of changed atoms with the rest of the enzyme, water, and S or TS. Therefore, $\Delta G_i = \Delta G_{ia} + \Delta G_{ib}$ for any particular atom that we change. We also make the assumption that the change in intragroup energies is equal in the different environments:

$$\Delta G_{4a} = \Delta G_{5a} = \Delta G_{6a}$$

$$\Delta G_{1a} = \Delta G_{2a} = \Delta G_{3a}$$

Finally, we are left with

$$\Delta\Delta G^*_{bind} = \Delta G_{5b} - \Delta G_{2b} - \Delta G_{4b} + \Delta G_{1b}$$

$$\Delta\Delta G^*_{cat} = \Delta G_{2b} - \Delta G_{3b} - \Delta G_{5b} + \Delta G_{6b}$$

In the simulations reported here, we assumed that $\Delta G_{1b} = \Delta G_{4b}$. We made this assumption because we could not calculate a realistic estimate of the difference in interactions of the perturbed atoms with the rest of the protein between the native and mutant structures. The problems were caused by large-scale side-chain movements because of the lack of substrate, both with and without solvent present. Even so, this is probably a reasonable assumption given that the environment around a particular residue is very similar in the two structures.

Computational Details. We employed the windowing method of perturbation to calculate free energies, which involves breaking up the perturbation into discrete steps (windows), as described by Singh et al.[10] Each progression from the unperturbed structure to the perturbed state, for the various simulations described below, was carried out with 5–21 windows; 200 equilibration steps and 400 steps of data collection were performed at each window, with a step size of 1 fs. Thus, the total time course for each perturbation was between 3 and 12.6 ps; different simulation times were used to ensure that the calculated free energies were independent of the length of time for the conversion. We were limited to fairly short simulation times. The structures drifted from their starting configurations during long simulations, particularly when we changed charges critical for maintaining side-chain or substrate orientations. The length of time for each simulation used here represents a compromise between minimizing hysteresis and attaining sufficient sampling. Only those residues within 10 Å of residue 165 were allowed to move. SHAKE[16] was used for all bonds, and all free energies were calculated at 300 K. A linear distance-dependent dielectric constant ($\epsilon = r_{i,j}$, where r is the intercharge separation between atoms i and j) and a 10-Å nonbonded cutoff were used for the calculations.

The reported free energy changes represent the average of at least two independent simulations. The uncertainties quoted with the average free energies are not true uncertainties but actually reflect the hysteresis within a particular run and between different runs. For each simulation from the unperturbed to the perturbed charge, we calculated two free energy changes, one for forward-looking sampling at each window and one for backward-looking sampling. The uncertainties reported here are the largest difference between either forward and backward sampling free energy changes or calculated free energy changes from different runs. Currently there is no way to rigorously determine the uncertainties for free energies calculated with this method.

Generation of Structures. We performed calculations on four TIM models with substrate: (1) wild-type TIM (Glu 165) with noncovalently bound DHAP; (2) mutant TIM (Asp 165) with noncovalently bound DHAP; (3) wild-type TIM with covalently bound DHAP; and (4) mutant TIM with covalently bound DHAP. The model for the wild-type noncovalent enzyme–substrate complex was the final structure, after 10.5 ps of molecular dynamics at 300 K, reported in an earlier study.[17] (This earlier study used the refined crystal coordinates of chicken muscle triosephosphate isomerase as the starting structure for molecular dynamics.[4,5]) The mutant structure was obtained by replacing Glu 165 with Asp, maintaining the original wild-type side-chain orientation. Another orientation of residue 165 was also used to test the dependence of the calculated free energy changes on the structure. This orientation was generated during a trial simulation aimed at perturbing Glu into Asp directly. Standard united-atom parameters (hydrogens on carbon atoms are incorporated into the van der Waals radius of the carbon) were used for the TIM dimer.[18] All structures contained the appropriate counterions on charged surface residues; however, explicit solvent molecules were not present. Structures were further equilibrated, to different extents but up to 7.5 ps, prior to perturbation calculations to ensure that the calculated free energies were not excessively dependent on starting structure. The covalent complexes were constructed, from preequilibrated noncovalent complexes, by imposing a covalent bond between the *pro-R* hydrogen of the substrate (H1R) and a carboxyl oxygen of residue 165 (O2 of Glu or Asp). (See Figure 3.) The resulting structures were then equilibrated for 1–5 ps at 300 K.

The partial charges for DHAP were determined in a single-point 4-31G* ab initio calculation[17] with the refined crystal coordinates of Banner et al.,[4,5] by use of the UCSF-G80 electrostatic potential fitting routine.[19] The substrate charges for the covalent enzyme–substrate complex were based on the gas-phase transition structure constructed by Alagona et al.,[20] with the addition of a phosphate group. Two nonstandard AMBER atom types were assigned for DHAP covalently bound to TIM. The parameters for the new atom types, TC for C1 and TH for the *pro-R* hydrogen, are given in Table I; all other substrate atoms were assigned standard all-atom parameters.[21]

(16) Ryckaert, J.; Ciccotti, G.; Berendensen, H. J. C. *J. Comput. Phys.* **1977**, *23*, 327.
(17) Brown, F. K.; Kollman, P. A. *J. Mol. Biol.* **1987**, *198*, 533.
(18) Weiner, S. J.; Kollman, P. A.; Case, D. A.; Singh, U. C.; Ghio, C.; Alagona, G.; Profeta, S., Jr.; Weiner, P. *J. Am. Chem. Soc.* **1984**, *106*, 765.
(19) Singh, U. C.; Kollman, P. A. *J. Comput. Chem.* **1984**, *5*, 129.
(20) Alagona, G.; Desmeules, P.; Ghio, C.; Kollman, P. A. *J. Am. Chem. Soc.* **1984**, *106*, 3623.
(21) Weiner, S. J.; Kollman, P. A.; Nguyen, D. T.; Case, D. A. *J. Comput. Chem.* **1986**, *7*, 230.

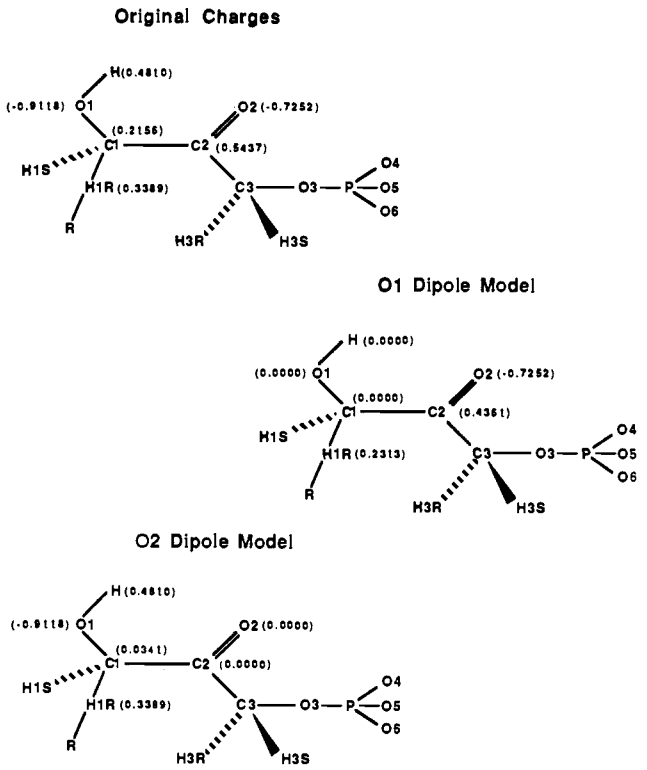

Figure 3. Models for perturbing charges and hydrogen bond dipoles in substrate (DHAP). The structures shown are for DHAP covalently bound to TIM through O2 of Glu or Asp (here represented as R). Partial charges are given in parentheses. The perturbed charges are explicitly shown here. All other charges are given in Table II.

Table I. Parameters for Atom Types TC and TH[a]

Bond Parameters

bond	K_r	r_{eq}
TC–TH	331.0	1.10
TC–C	317.0	1.43
TH–O2	331.0	1.60

Angle Parameters

angle	K_θ	θ_{eq}	angle	K_θ	θ_{eq}
TH–TC–OH	135.0	109.5	O2–TH–TC	0.0	179.9
O2–TC–C	0.0	109.5	TC–C–CT	70.0	118.6
O2–TC–TH	0.0	1.0	TH–TC–HC	135.0	109.5
O2–TC–HC	0.0	109.5	OH–TC–C	63.0	109.5
O2–TC–OH	0.0	109.5	TC–C–O	80.0	120.4
TC–O2–C	0.0	120.0	TC–OH–HO	55.0	108.5
TH–TC–C	135.0	109.5	C–O2–TH	70.0	120.0

Torsion Parameters

torsion	$V_n/2$	γ	n
X–TC–TH–O2	0.0	0.0	2.0
X–O2–TC–X	0.0	0.0	3.0
OH–TC–C–X	20.0	180.0	2.0

Nonbonded Parameters

atom	R	ϵ
TH	0.10	0.000

[a] Nonstandard atom type parameters that are the same as the standard parameters are not listed here (e.g., when TC and CT and when TH and HC have the same parameters). See ref 18 for standard parameters. The parameters are in the following units: K_r = kcal/mol·Å^2; r_{eq} = Å; K_θ = kcal/mol·rad^2; θ_{eq} = degrees; $V_n/2$ = kcal/mol; γ = degrees, R^* = Å; and ϵ^* = kcal/mol.

Description of Protein Residue Perturbations. Potential hydrogen-bonding sites of specific amino acid residues in the active site and portions of the substrate were removed by zeroing the charge on the hydrogen and/or oxygen atoms. The perturbed groups fall into three categories:

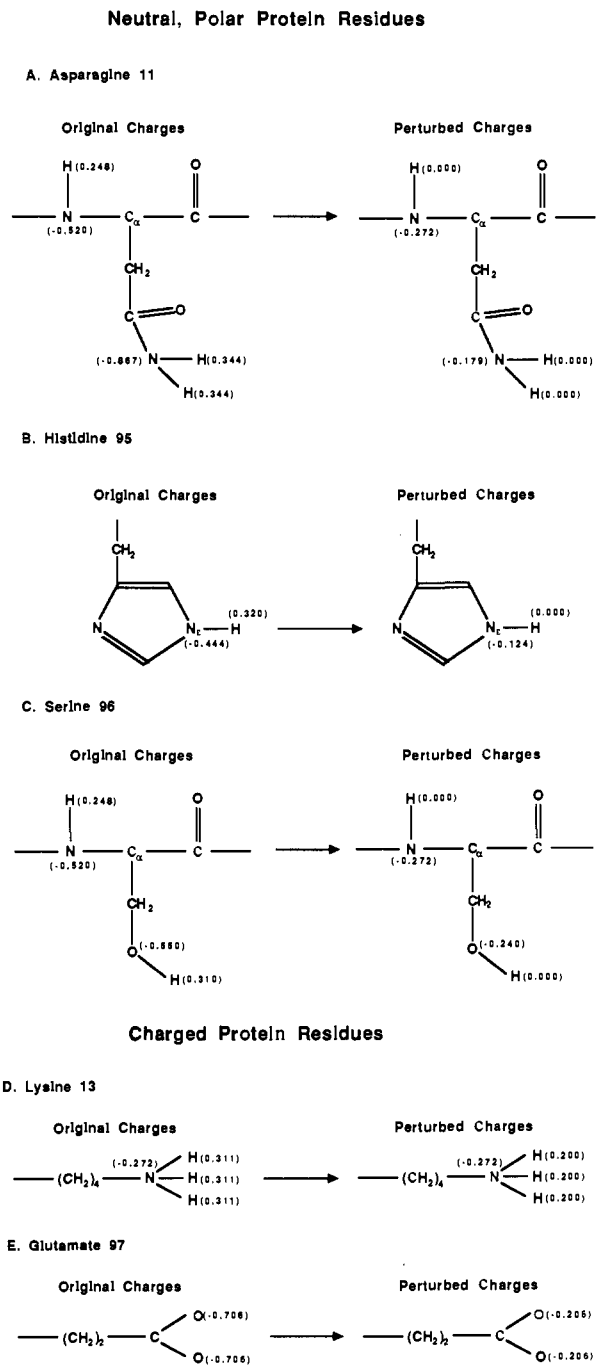

Figure 4. Models for perturbing active site hydrogen bond dipoles and charges of TIM. Partial charges are given in parentheses. All perturbed charges and the pertinent original charges are depicted.

neutral, polar protein residues; charged protein residues; and the substrate.

(A) Neutral, Polar Protein Residues. In the case of the neutral, polar residues, overall charge neutrality was maintained in going from the perturbed to the unperturbed state. To maintain charge neutrality, it was necessary to change the charges of some atoms covalently connected to the potential hydrogen-bonding atoms. Three residues fall into this group of perturbed residues: Asn 11, His 95, and Ser 96. The pertinent original charges and all-perturbed charges for these residues are given in Figure 4.

(B) Charged Protein Residues. The perturbation of the charged residues involved neutralizing a full charge, and the changes were localized to the actual atoms of interest. Two fully charged residues in the active site were neutralized—Lys 13 and Glu 97 (Figure 4). The perturbation of Glu 97 was straightforward and involved only changing the charges on the oxygens. The determination of interactions between lysine 13 and its environment, on the other hand, was complicated by the strong interactions between the ϵ-amino group and the phosphate group of DHAP.

Table II. Original and Perturbed Partial Charges for DHAP Dipoles in Noncovalent and Covalent Complexes with TIM[a]

atom[a]	atom type[b]	original charge	perturbed charge: O1 dipole	perturbed charge: O2 dipole	perturbed charge: O1/O2
			Noncovalent		
H	HO	0.4452	0.0000	0.4452	0.0000
O1	OH	−0.7955	0.0000	−0.7955	0.0000
C1	CT	0.2966	0.0000	0.2966	0.0000
H1R	HC	−0.0150	−0.0150	−0.0150	−0.0150
H1S	HC	−0.0125	−0.0125	−0.0125	−0.0125
C2	C	0.6879	0.6879	0.0000	0.0000
O2	O	−0.6367	−0.6367	0.0000	0.0000
C3	CT	0.1714	0.1714	0.1714	0.1714
H3R	HC	0.0119	0.0119	0.0119	0.0119
H3S	HC	0.0121	0.0121	0.0121	0.0121
O3	OS	−0.5971	−0.5971	−0.5971	−0.5971
P	P	1.4452	1.4452	1.4452	1.4452
O4	O2	−1.0045	−1.0045	−1.0045	−1.0045
O5	OH	−1.0045	−1.0045	−1.0045	−1.0045
O6	OH	−1.0045	−1.0045	−1.0045	−1.0045
total charge:		−1.9999	−1.9463	−2.0512	−1.9975
			Covalent		
H	HO	0.4810	0.0000	0.4810	0.0000
O1	OH	−0.9118	0.0000	−0.9118	0.0000
C1	TC	0.2156	0.0000	0.0341	0.0000
H1R	TH	0.3389	0.2313	0.3389	0.0041
H1S	HC	0.0041	0.0041	0.0041	0.0041
C2	C	0.5437	0.4361	0.0000	0.0000
O2	O	−0.7252	−0.7252	0.0000	0.0000
C3	CT	0.2764	0.2764	0.2764	0.2145
H3R	HC	−0.0286	−0.0286	−0.0286	−0.0286
H3S	HC	−0.0286	−0.0286	−0.0286	−0.0286
O3	OS	−0.5971	−0.5971	−0.5971	−0.5971
P	P	1.4452	1.4452	1.4452	1.4452
O4	O2	−1.0045	−1.0045	−1.0045	−1.0045
O5	OH	−1.0045	−1.0045	−1.0045	−1.0045
O6	OH	−1.0045	−1.0045	−1.0045	−1.0045
total charge:		−1.9999	−1.9999	−1.9999	−1.9999

[a] See Figure 3. [b] See ref 17.

To separate the interactions between Lys 13 and non-phosphate portions of the substrate, the phosphate group, and other active site residues, we included various atoms in the perturbing group, which remained unchanged during the simulation. Only results for the perturbation of Lys 13 in the covalent complex are reported. The structural consequences of changing the Lys charges were too drastic in the noncovalent structure to provide meaningful results.

Four separate perturbation calculations were performed to explore interactions between Lys 13 and its environment: (1) a 30% decrease in the partial charges of the N_ϵ hydrogens; (2) a 30% decrease in the partial charges of the hydrogens and the definition of the entire substrate as part of the perturbing group (without any of its parameters changing); (3) a 30% reduction in the charge of the hydrogens and inclusion of the phosphate group as part of the perturbing group; and (4) the partial charges on the hydrogens were zeroed and the phosphate group was part of the perturbing group. The first perturbation is shown schematically in Figure 4. The decrease in hydrogen charge of 30% was arbitrary. Our concern was to calculate free energies of reasonable magnitude (e.g., not too large) so that the uncertainties were not too large.

Substrate Perturbations. In addition to perturbing active site residues, portions of the substrate were perturbed to determine their interactions with the enzyme active site. Figure 3 shows the original and perturbed charges for DHAP in the covalent complex. (See Table II for the complete set of charges.) The O1 dipole model involved perturbing the dipole resulting from the hydroxyl group at C1. The charges of other atoms in the substrate were also altered to maintain the original overall charge. The O2 dipole model involved zeroing the charges of the carbonyl group. (See Figure 2 for an illustration of the O2 dipole change.) The combined O1/O2 dipole model entailed the simultaneous perturbation of both dipoles. The various charges for perturbation of the substrate in the noncovalent complexes are shown in Table II and are analogous to those described above.

Results

Neutral, Polar Protein Residues. (A) Asparagine 11. The free energy changes for zeroing the backbone N−H and side-chain N−H dipoles of Asn 11 (Figure 4A) are given in Table III. Asn 11 interacts strongly with its environment in all four structures. The wild-type noncovalent complex is stabilized by 2 kcal/mol over the mutant complex (12.1 vs 10.1 kcal/mol, Table III). This difference appears to be due to less repulsive interactions, between one of the Asn side-chain amides hydrogens and the side-chain hydrogens of Gln 64, in the wild-type complex than in the mutant complex. The distances between the hydrogens were over 0.8 Å shorter in the mutant structure than in the wild-type enzyme; this difference could easily account for a 2 kcal/mol difference in the calculated ΔG. The interactions between the substrate atoms and Asn 11 appear to be very similar in the two structures. As can be seen in Figure 5, the orientations of Asn 11 in the wild-type enzyme and in the mutant are essentially the same; for example, the distance between a side-chain amide hydrogen and O1 of the substrate in the noncovalent wild-type and mutant complexes is 1.85 and 1.82 Å, respectively (Table VI). The free energy changes

Table III. Free Energy Changes upon Perturbing Charges and Hydrogen Bond Dipoles in Protein (kcal/mol)

protein model	substrate model	ΔG[a]
Asparagine 11: NH and NH_2 (Figure 4A)		
Glu 165	noncovalent	12.1 ± 0.1
Asp 165	noncovalent	10.1 ± 0.2
Glu 165	covalent	14.9 ± 1.2
Asp 165	covalent	14.2 ± 1.3
Histidine 95: N_ϵ−H (Figure 4B)		
Glu 165	noncovalent	4.4 ± 0.2
Asp 165	noncovalent	4.8 ± 0.4
Glu 165	covalent	4.2 ± 0.4
Asp 165	covalent	3.5 ± 1.7
Serine 96: NH and OH (Figure 4C)		
Glu 165	noncovalent	13.2 ± 0.7
Asp 165	noncovalent	11.0 ± 0.4
Glu 165	covalent	12.3 ± 1.0
Asp 165	covalent	12.9 ± 1.6
Glutamate 97: O1 and O2 (Figure 4E)		
Glu 165	noncovalent	23.7 ± 0.5
Asp 165	noncovalent	22.4 ± 0.3
Glu 165	covalent	19.7 ± 0.6
Asp 165	covalent	23.6 ± 4.0

[a] The free energy changes reported in this table conform to the formalism under Methods by noting the following: changes in the wild-type enzyme in the noncovalent complex represent ΔG_2; perturbation of the Asp mutant in the noncovalent complex corresponds to ΔG_5; free energies for the wild-type covalent complex represent ΔG_3; and changes in the mutant covalent complex correspond to ΔG_6.

Table IV. Free Energy Changes upon Perturbing Hydrogen Bond Dipoles of Lysine 13 (N_ϵ−H) and Portions of Substrate (kcal/mol)

perturbation	substrate model	protein model	ΔG[b]
(1) H charge 0.311 → 0.2[a]	covalent	Glu 165	28.4 ± 0.1
		Asp 165	31.1 ± 0.2
(2) H charge 0.311 → 0.2, substrate → substrate	covalent	Glu 165	3.2 ± 0.4
		Asp 165	2.2 ± 0.1
(3) H charge 0.311 → 0.2, phosphate → phosphate	covalent	Glu 165	11.0 ± 0.2
		Asp 165	4.9 ± 1.5
(4) H charge 0.311 → 0.0, phosphate → phosphate	covalent	Glu 165	26.1 ± 1.2
		Asp 165	10.3 ± 1.2

Differences between the Perturbations Above

difference	protein model	$\Delta\Delta G$	interaction
(1) − (2)	Glu 165	25.2	Lys 13 and substrate
	Asp 165	28.9	
(1) − (3)	Glu 165	17.5	Lys 13 and phosphate portion of substrate
	Asp 165	27.0	
(3) − (2)	Glu 165	7.7	Lys 13 with substrate minus phosphate group
	Asp 165	1.9	

[a] See Figure 4D. [b] The free energy changes reported here for the wild-type complex correspond to ΔG_3 in the free energy cycle given under Methods. The values for the mutant enzyme represent ΔG_6.

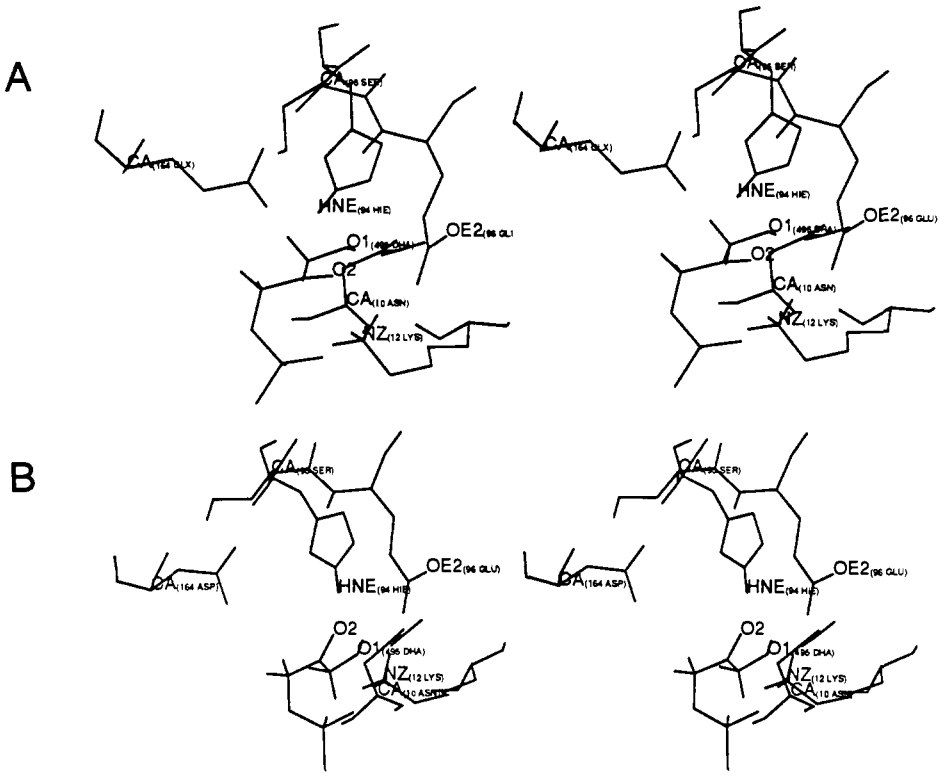

Figure 5. Stereoviews of the active site region of noncovalent DHAP–TIM complexes. (A) Wild-type TIM (Glu 165) and DHAP. The structure was the starting structure for perturbation calculations and has been equilibrated at 300 K with MD. The numbering and labels are slightly different than in the text. Residue 164 (GLX) is Glu 165. Residue 495, DHA, is the substrate DHAP. The numbering of the residues differs from the numbering in the text by one: His 95 is His 94, Asn 11 is Asn 10, Ser 96 is Ser 95, Lys 13 is Lys 12, and Glu 97 is Glu 96 in this figure. (B) Mutant TIM (Asp 165) and DHAP. The structure was the starting structure for perturbation calculations (at 300 K). Residue 164 in this figure is Asp 165. The other residues are the same as described above.

Table V. Free Energy Changes upon Perturbing Charges and Hydrogen Bond Dipoles in Substrate (kcal/mol)[a]

protein model	substrate model	ΔG^b
	O1 Dipole	
Glu 165	noncovalent	2.8 ± 0.9/2.1 ± 0.8
Asp 165	noncovalent	1.5 ± 0.1/1.1 ± 0.5
Glu 165	covalent	−1.9 ± 0.2
Asp 165	covalent	−3.4 ± 0.9
	O2 Dipole	
Glu 165	noncovalent	6.8 ± 0.9/3.9 ± 0.4
Asp 165	noncovalent	6.2 ± 1.0/2.8 ± 0.9
Glu 165	covalent	9.4 ± 0.2
Asp 165	covalent	7.9 ± 0.5
	O1/O2 Dipole	
Glu 165	noncovalent	6.4 ± 1.2/7.8 ± 0.8
Asp 165	noncovalent	7.0 ± 0.7/8.0 ± 0.3
Glu 165	covalent	15.6 ± 0.6
Asp 165	covalent	1.9 ± 0.3

[a] See Figure 3. [b] Two free energy changes are listed for each noncovalent complex. The first represents the wild-type side-chain orientation of residue 165 (regardless of whether it is Glu or Asp), and the second refers to a slightly different orientation of residue 165 generated during a trial run aimed at perturbing Glu directly into Asp. Also, to conform to the formalism outlined under Methods, the free energy changes reported for the wild-type noncovalent structure represent ΔG_{ES}, those for the mutant noncovalent structure represent $\Delta G_{E'S}$, those for the wild-type covalent complex are ΔG_{ETS}, and those presented for the mutant covalently bound substrate structure represent $\Delta G_{E'TS}$.

Table VI. Distances (Å) between Active Site Residues for Wild-Type TIM and Mutant TIM (Asp 165)

residues involved	atoms involved[a]	noncovalent Glu[b]	noncovalent Asp[c]	covalent Glu[d]	covalent Asp[e]
Asn 11, substrate	HN_δ, O1	1.85	1.82	2.12	3.81
Lys 13, substrate	N_ϵ, O2	2.75	3.61	3.00	4.31
Lys 13, substrate	N_ϵ, O3	4.18	4.22	4.44	4.06
Lys 13, substrate	N_ϵ, O4	2.48	2.53	2.64	2.52
Lys 13, substrate	N_ϵ, O5	2.60	2.59	2.84	2.53
Lys 13, substrate	N_ϵ, O6	4.54	4.37	4.68	4.47
Lys 13, Glu(Asp) 165	N_ϵ, O2	5.51	6.91	7.10	7.07
His 95, substrate	HN_ϵ, O1	2.76	3.36	2.70	3.04
His 95, substrate	HN_ϵ, O2	2.21	1.70	2.43	1.76
His 95, substrate	HN_ϵ, O1H	2.26	2.55	2.10	2.27
His 95, Glu(Asp) 165	HN_ϵ, O2	1.78	4.46	4.47	4.61
Ser 96, Glu(Asp) 165	HOG, O1	1.72	2.48	2.20	1.77
Ser 96, Glu(Asp) 165	HN, O1	1.69	1.85	2.46	1.67
Glu 97, substrate	O2, O1H	3.87	4.66	5.28	6.70
Glu 97, Lys 13	O1, HN_ϵ	1.74	1.69	1.82	1.67
Glu(Asp) 165, substrate	O2, O2	3.26	4.40	4.16	4.31
Glu(Asp) 165, substrate	O1, O1	4.08	6.33	3.39	3.40
Glu(Asp) 165, substrate	O2, H1R	3.08	5.29	1.20	1.20
Glu(Asp) 165, substrate	O2, C1	3.54	5.51	2.70	2.70

[a] Where there is more than one choice for the distances involving hydrogens, the lowest distance is reported. [b] Figure 5A. [c] Figure 5B. [d] Figure 6A. [e] Figure 6B.

for perturbing Asn 11 in the covalent structures are essentially the same, 14.9 vs 14.2 kcal/mol (Table III), although Asn 11 makes a hydrogen bond with O1 of the substrate in the wild-type complex but shifts to O2 in the mutant complex.

(B) Histidine 95. The free energies for perturbing the hydrogen bond donor site of histidine 95 are unfavorable, which is consistent with the suggestion that it interacts favorably with the substrate by providing a positive electrostatic environment. However, our results indicate that the hydrogen bond interacts in a similar manner in all four of the structures (all of the free energies are approximately 4 kcal/mol, Table III). In the absence of discrimination between wild-type and mutant TIM, the drop in activity cannot be explained in terms of differential histidine interactions. As mentioned above, these free energies represent interactions between His 95 and its environment. So, differences between the free energies for perturbation of wild-type and mutant

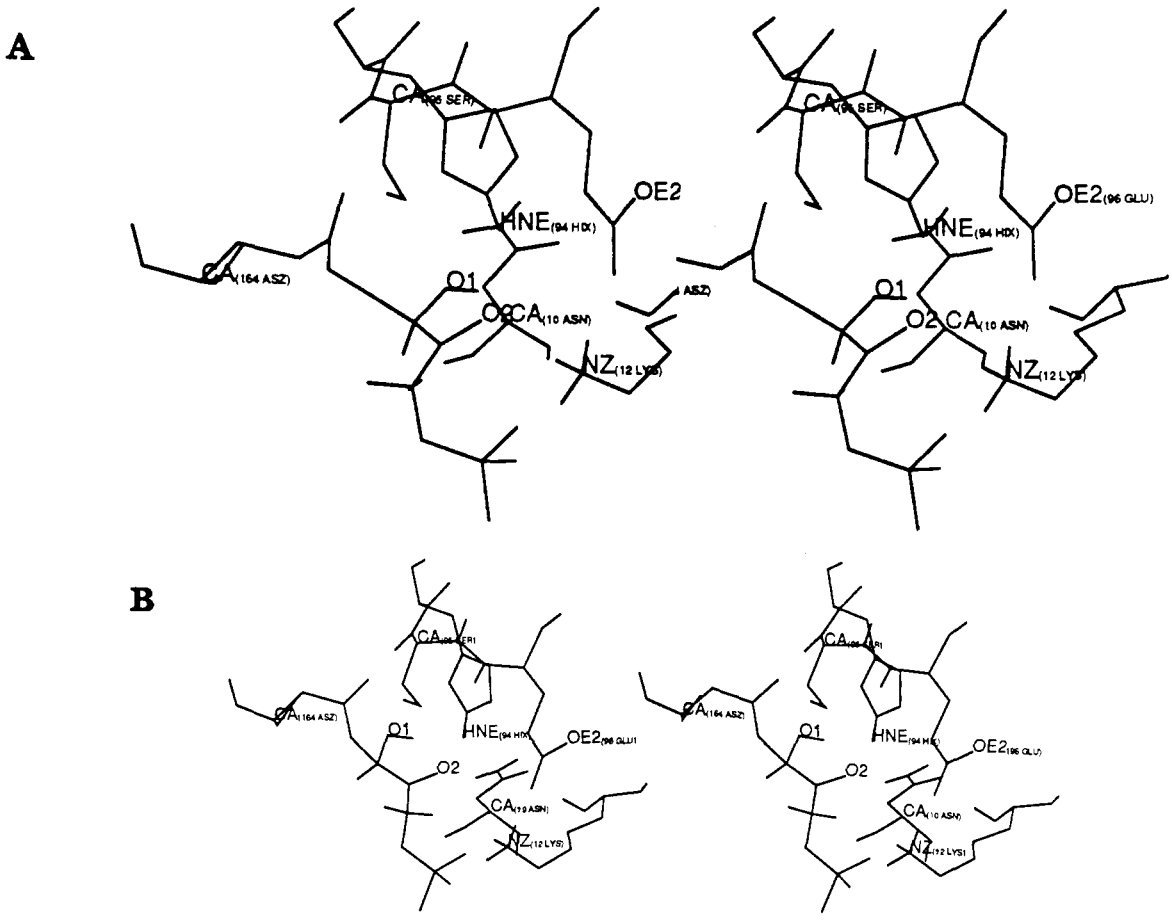

Figure 6. Stereoviews of active site regions of covalent DHAP–TIM complexes. (A) Wild-type TIM (Glu 165) and DHAP. The structure was the starting structure for perturbation calculations and has been equilibrated at 300 K with MD. The labeling is essentially the same as in Figure 5 except for the following differences: residue 164, ASZ, is Glu 165 covalently linked through O2 to H1R of the substrate. (B) Mutant TIM (Asp 165) and DHAP. The structure was the starting structure for perturbation calculations. The labeling is the same as described above. Residue 164 (ASX), however, represents Asp 165 covalently linked to DHAP.

structures can be due to any number of interactions. In some cases perturbation of different structures can yield different energetic contributions while maintaining the same overall free energies. It appears as though this might be the case with the His 95 perturbations. For example, the HN_ϵ–O2 (of the substrate) distances in the Glu structures (noncovalent 2.21 Å, covalent 2.43 Å) are longer than in the Asp structures (noncovalent 1.70 Å, covalent 1.76 Å). (See Table VI.) This might suggest that His 95 of the Asp 165 structure would better stabilize the transition state, but the geometry of the hydrogen bond is less than optimal. (Compare structures A and B of Figure 6.) Also, HN_ϵ of His 95 interacts more strongly with O1 in the wild-type structure than in the mutant structure. Even though it appears that His 95 is in a better position to stabilize O2 of the substrate in the mutant transition structure (in terms of distances between HN_ϵ and O2 of the substrate), there are compensating interactions in the wild-type structure that result in similar overall free energies for perturbation of the two covalent structures. It may be important to maintain His 95 poised between O1 and O2, which the wild type does very effectively and the mutant does not (Figure 6 and Table VI).

(C) Serine 96. Serine 96 interacts strongly with its environment in all four structures. The free energy for this interaction in the wild-type noncovalent complex is 2.2 kcal/mol more favorable than in the mutant complex (13.2 vs 11.0 kcal/mol, Table III). The environment around Ser 96 is very similar in the two noncovalent structures with the exception that Ser 96 is in a more favorable position to form a hydrogen bond with O1 of Glu 165 in the wild-type structure. The distance between the hydroxyl proton of Ser 96 and O1 of residue 165 is 0.8 Å longer for mutant TIM than for wild-type TIM (Table VI); there is less than a 0.2-Å difference between the Ser HN and O1 distances. It is important to note that the calculated free energies are a measure of the interactions between the perturbed residue and the rest of the protein as well as the substrate. Therefore, although our intention is to interpret the free energies in terms of probable molecular interactions, we need structural confirmation that the proposed hydrogen bonds exist.

Charged Protein Residues. (A) Lysine 13. The results for the various lysine 13 perturbations are presented in Table IV. The first perturbation represents the interaction of Lys 13 with its environment, including the entire substrate. Lys 13 stabilizes the Asp 165 transition structure by almost 3 kcal/mol over the wild-type structure (31.1 vs 28.4 kcal/mol). The free energies for the second perturbation (H charge 0.311 → 0.200 and substrate → substrate) are a measure of interactions between Lys 13 and other TIM residues but do not include interactions with the substrate. In this case, the wild-type covalent complex is stabilized by approximately 1 kcal/mol, although both values are fairly low. The third perturbation (H charge 0.311 → 0.200 and phosphate → phosphate) represents interactions between Lys 13 and other TIM residues in the active site and all of the substrate atoms except the phosphate group. This interaction stabilizes the wild-type covalent complex over the mutant structure by 6 kcal/mol (11.0 vs 4.9 kcal/mol).

Table IV also contains free energy changes for interactions between Lys 13 and portions of the substrate. The difference between the free energy changes ($\Delta\Delta G$) for perturbation 1 (that is, Lys interactions with the environment) and perturbation 2 (Lys interactions with everything but the substrate) represents the free energy of interaction between Lys 13 and DHAP. The free energies for this interaction, for both the wild-type and mutant covalent structures, are large; the interaction is almost 4 kcal/mol more favorable for the mutant. The difference between pertur-

bations 1 and 3 (Lys interactions with everything but the phosphate portion of the substrate) reflects interactions between Lys 13 and the phosphate group of DHAP. This interaction is much stronger for mutant TIM (by approximately 10 kcal/mol) than for the wild-type enzyme. The difference between perturbations 2 and 3 is a measure of the interactions between Lys 13 and the nonphosphate portion of the substrate. For this case, the wild-type covalent complex is favored by almost 6 kcal/mol compared to the mutant structure. These results indicate that the substrate interacts strongly with the lysine in the mutant transition structure, although in a nonproductive manner (e.g., Lys 13 interacts strongly with the phosphate group instead of polarizing O2). As can be seen in Table VI, the N_ϵ–O2 distance is 1.3 Å greater for the mutant transition structure than for the wild-type structure. In contrast, the ϵ-amino group of Lys 13 is closer to the phosphate group in the mutant structure. (See relevant distances in Table VI and compare structures A and B of Figure 6.)

(B) Glutamate 97. The free energy change for neutralizing fully charged Glu 97 in the noncovalent wild-type complex is 1.3 kcal/mol higher than in the mutant complex. The added stability in the wild-type case may be due to more effective interactions between O2 of Glu 97 and O1H of the substrate (this distance is ~0.8 Å shorter in the wild-type structure compared to that in the mutant, Table VI). This Glu 97 substrate interaction is the only interaction that we found to be very different between the two structures. Even in the wild-type enzyme this distance is fairly large, and Glu 97 does make closer contact with Lys 13 than with the substrate, but the distances and side-chain orientations are essentially the same in the wild-type and mutant structures. (The distance between Glu 97 O1 and $N_\epsilon H_1$ of Lys 13 is 1.74 Å for the wild type compared to 1.69 Å for the mutant, Table VI.)

The free energy changes for perturbing the O1 and O2 charges of Glu 97 in the covalent structures differ by 3.9 kcal/mol, with the mutant structure favored over the wild-type complex (Table III). It is not clear whether this is a real effect, though. Unfortunately, the perturbation simulations of the mutant complex were not stable, yielding a large uncertainty in this value. Given the large uncertainties, the two values are essentially the same.

Substrate Perturbations. We also examined interactions in the active site from the point of view of the substrate by perturbing catalytically important portions of the molecule. Free energy changes for perturbing the O1 dipole of the substrate within both the Glu 165 and Asp 165 covalent structures are favorable (Table V). The free energies for removing the O2 dipole in both covalent structures are fairly large and positive. The Glu covalent complex gains 9.4 kcal/mol in stabilization energy from the O2 dipole and is destabilized 1.9 kcal/mol by the O1 dipole, yielding a net 7.5 kcal/mol stabilization due to the environment around O1 and O2 of the substrate. The analogous overall stabilization free energy for the Asp covalent complex is 4.5 kcal/mol. Thus, on the basis of the O1 and O2 dipoles, the Glu transition state model is stabilized by 3 kcal/mol over the Asp covalent complex.

The free energies for the O1 dipole perturbation in the noncovalent wild-type and mutant complexes are essentially the same. Two values are given for each enzyme–substrate complex. The first value represents the wild-type side-chain orientation of residue 165 (regardless of whether it is Glu or Asp), and the second represents a slightly different orientation of residue 165 generated during a trial run aimed at perturbing Glu directly into Asp. We can see in Table V that there is some dependence on structure. For example, the free energies for disappearance of the O2 dipole differ by 2.9 kcal/mol in the noncovalent wild-type complexes. If the same orientations are compared for the wild-type and mutant structures for a particular perturbation, however, the free energies are within the uncertainties. Despite the conformational dependence of the free energies, like orientations result in similar free energies for the wild type and the mutant. Therefore, both mutant and wild-type substrate binding appear to be affected to the same degree by loss of the O1 and O2 dipoles.

The results for the simultaneous "disappearance" of both the O1 and O2 dipoles for the covalent complexes are not the sum of the single perturbations (Table V). To maintain the total charge of the substrate constant, we altered the charges of other substrate atoms. Different atoms were perturbed, and to different extents, in the transition state models. Hence, there is no reason to expect the results to be additive. Another explanation for the nonadditivity is that the position of the substrate changes during the perturbation simulation in the absence of the electrostatic interactions that aid in anchoring the substrate in the active site. The difference between the free energies for the wild-type and mutant structures further illustrates the favorable positions of the residues, which stabilize the O1 and O2 dipoles, in the wild-type structure. Our results show that the mutant stabilizes the O1 and O2 dipoles much less efficiently than native TIM. However, the difference between the two is large and cannot be correlated in a quantitative way with the experimentally observed 4 kcal/mol difference in k_{cat}.

Discussion

Our models for the noncovalent substrate–mutant TIM (Asp 165) complex, after equilibration, show the substrate interacting with most active site residues to the same extent as in the wild-type structure, instead of being pulled in toward Asp 165. (Compare structures A and B of Figure 5.) For example, the distance between O2 of Glu or Asp and the *pro-R* hydrogen of the substrate is much shorter for wild-type TIM than for the mutant TIM (3.08 and 5.29 Å, respectively). In contrast, the distances between the phosphate oxygens and the lysine group are essentially the same (Table VI). The calculated free energies for perturbing portions of the substrate DHAP in the active site of the wild-type and mutant noncovalent complexes are nearly the same when like orientations are compared (Table V), suggesting that substrate binding is not significantly altered upon mutation of Glu 165 to Asp providing that other substrate–enzyme interactions do not differ greatly. This is in agreement with the experimental results.

The results for perturbing active site protein residues are a bit more ambiguous because there can be many compensating interactions for any particular interaction that we observe. Therefore, any comparison to the experimental results is tenous unless all possible interactions in the active site are evaluated, since $\Delta\Delta G_{bind}$ and $\Delta\Delta G_{cat}$ correspond to the effect of all of the individual free energy changes. The perturbations of the substrate should be measures of enzyme–substrate interactions that can be related, at least qualitatively, to the experimental results while the protein residue perturbations are most useful for ascertaining which residues are important for substrate binding and catalysis. We found differences between the free energy changes of interaction for charge perturbations of Asn 11, Ser 96, and Glu 97 in the noncovalent complexes, and we have suggested possible reasons for the differences, which could be tested experimentally.

Upon mutation of Glu 165 to Asp, k_{cat} drops by approximately 3 orders of magnitude.[1] At least three explanations for the drop in activity of the mutant have been proposed. Alagona et al.[22] suggest two plausible interpretations of the lower catalytic activity of the Asp 165 mutant. They show that a small (0.3 Å) change in the C···O distance in the transition state (normally 2.6 Å) could result in a 4 kcal/mol higher barrier to proton transfer from the substrate to the enzymic carboxylate. They also note that if the Asp 165 mutant is able to achieve the 2.6-Å distance without extra stereochemical strain, the increase in the free energy of activation might be rationalized in terms of less effective interactions between the substrate in the covalent complex and electrophilic groups in the active site. The focus of this paper is the second possibility for the lower activity of the Glu 165 → Asp mutant suggested by Alagona et al.: less effective interactions between some electrophilic group(s) in the active site and the substrate. We forced the substrate and enzyme to adopt transition structures by imposing a covalent bond between the two (Figure 3) and evaluated various interactions in the wild-type and mutant transition structures without regard to how these structures might actually be attained. We cannot simulate bond-making steps using the approach outlined here; therefore, the question of the distance

(22) Alagona, G.; Ghio, C.; Kollman, P. A. *J. Mol. Biol.* **1986**, *191*, 23.

between the attacking carboxylate oxygen of Glu or Asp and the *pro-R* hydrogen remains a possible source of the drop in activity of the mutant enzyme. Nevertheless, we suggest that less effective interactions between Lys 13 and the substrate in the transition state structure of the Asp 165 mutant might explain the observed drop in catalytic activity.

The free energies reported here for perturbing the charges of the other active site residues, besides Lys 13, in the wild-type and mutant transition structures are all within the reported uncertainties (Table III). The only striking difference between the structures is seen for the Lys 13 perturbations (Table IV). While the results for perturbing Lys 13 are not directly comparable to the substrate perturbations, they offer a plausible explanation for why the mutant is catalytically less effective than the wild-type enzyme, but this does not rule out other interactions. By looking at $\Delta\Delta G$ for the Lys 13 perturbations, we were able to separate the interactions between this residue and the catalytic portion of the substrate and the phosphate group. On the basis of these results, Lys 13 interacted strongly with the substrate in a nonproductive manner in the mutant, by strong interactions with the phosphate group but not the catalytically important portions of the substrate.

Raines et al.[9] offer an alternative explanation for the decrease in "transition state binding" based on the geometry of proton abstraction by the enzymic base. Earlier, Gandour[23] postulated that a carboxylate group is an approximately 100-fold better catalyst when the proton is transferred in a syn orientation (to both carboxylate oxygens simultaneously) than in an anti orientation (to only one carboxylate oxygen). Given this argument, k_{cat} would be expected to decrease if Asp 165 of the mutant were to abstract a substrate proton in an anti orientation. Current theoretical approaches cannot definitively establish which of the three explanations is correct, or indeed if some other explanation is.

Nonetheless, our interpretation of the drop in activity of the mutant enzyme could be tested by site-specific mutation of the lysine residue. We would suggest that replacing Lys 13 by Arg might result in an increase in activity of the Asp 165 mutant. The longer side chain of Arg may facilitate stabilization of the substrate by this mutant. Furthermore, in the absence of unforseen complications, we would expect a single Lys 13 → Ala mutant (Glu 165, Ala 13) and the corresponding double mutant (Asp 165, Ala 13) to have comparable, low activities. Alanine would be unable to stabilize the substrate, if the positive charge in this position is indeed crucial.

The nature of the intermediate—enediol, or enediolate—has not been definitively established. Rose et al.[24] argue in favor of the enediol. On the other hand, the effectiveness of phosphoglycolate[25] in inhibiting TIM suggests that the enediolate plays an important role at some stage of the reaction. One could imagine protonation of the enediolate by water with a low activation energy.[20] The covalent models examined in this study employ an enediolate. If the rate-limiting transition state of the reaction involves formation of the enediol, then the models we have constructed are not appropriate for interpreting the experimental data relating to catalysis (k_{cat}). However, if, as mentioned above, the enediolate is important and is rapidly protonated (compared to formation of the enediolate) by solvent, then our models are relevant. (For a more thorough discussion see ref 20.)

Another limitation of our models is that solvent is not explicitly present. We attempted to compensate for this by using a distance-dependent dielectric function; however, this dielectric model leads to an overestimation of the effect of changing a full charge. The commonly accepted value of the internal dielectric constant of the protein interior is between 1 and 5.[27] Recent experimental work suggests, however, that the effective dielectric constant of the protein interior is between 40 and 50.[28-30] The use of $\epsilon = r_{ij}$, then, severely underestimates the influence of the solvent on the dielectric constant of proteins. The simple addition of solvent and the use of a dielectric constant of unity would probably still result in a poor model for the heterogeneous dielectric environment within the protein. In addition, it is not appropriate to construct such an elaborate model given the low resolution of the available X-ray structures. Despite these shortcomings, the importance of this study lies in the development of the free energy component analysis, in which one perturbs specific portions of the enzyme or substrate. This method can give qualitative insight into the residues that are important in binding and catalysis. Thus, free energy calculations can be useful in the qualitative way described here as well as the quantitative approaches used in the studies by Bash et al.[12] and Rao et al.[13]

Knowles and co-workers have engineered other interesting mutants, whose properties we can discuss in terms of the results presented here. Asp 165, Pro 96—a pseudorevertant of the relatively inactive Asp 165, Ser 96 single mutant—is a significantly better catalyst than the single mutant.[7] Our results suggest that Ser 96 forms hydrogen bonds of similar strength with both native TIM and the Asp 165 mutant in the covalent structures, although we do see a difference for the noncovalent complexes. The calculated $\Delta\Delta G^*_{cat}$ contribution from Ser 96 is 2.8 kcal/mol (favoring the Asp mutant), but this value is within the sum of the uncertainties, making any quantitative arguments tenuous. Therefore, the strength of these hydrogen bonds probably cannot be used to explain the relative catalytic activities of the Glu 165, Pro 96 and the Asp 165, Pro 96 mutants.[7] Mutating Ser 96 to Pro in the native enzyme reduces k_{cat} such that both Pro 96 proteins (that is, Glu and Asp in position 165) have comparable activities. The Pro 96 mutants appear to exert their effect by changing the relative orientations of the key catalytic groups at positions 165, 95, and 13. A change in these orientations can be deleterious, as in the case of the native structure. But it may be advantageous to alter the Asp 165 enzyme in order to bring His 95 or Lys 13 into a better orientation to stabilize the transition structure.

It is interesting to note that a pseudorevertant of His 95 → Asn 95 is the double mutant Asn 95, Pro 96.[7] That Pro 96 can revert mutations at both positions 95 and 165 is consistent with the idea that the relative orientation of these groups is critical for catalysis. Actual simulations of the Pro 96 mutants are required to assess the speculations presented above on the low activities of the Asp 165 and Asn 95 enzymes and the partially restored activity of the Asp 165, Pro 96 and the Asn 95, Pro 96 structures. We have performed molecular dynamics simulations of these mutants, and preliminary analysis indicates that Pro 96 does indeed affect the orientation of other active site residues (unpublished results).

Conclusions

Free energy perturbation calculations can give interesting insights into the effects of amino acid substitutions on both substrate binding and catalysis. We have shown how a free energy component analysis, in which one perturbs the properties of individual groups on the enzyme or ligand, yields detailed information, albeit qualitative, about the specific interactions important in enzyme action. In the specific application studied here, we have used a simple model without explicit inclusion of solvent and a distance-dependent dielectric constant to compensate for the lack of solvent. Thus, we have not implemented the free energy component analysis in as rigorous a fashion as might have been warranted if we had a better X-ray structure and the reaction had not involved a highly charged substrate. Nonetheless, we suggest that the free energy component analysis tool can be as useful and insightful as energy component analysis has been in molecular mechanics studies.[31-33]

(23) Gandour, R. D. *Bioorg. Chem.* **1981**, *10*, 169.
(24) Iyengar, R.; Rose, I. *Biochemistry* **1981**, *20*, 1223, 1229.
(25) Wolfenden, R. *Nature* **1969**, *223*, 704.
(26) Deleted in proof.
(27) Pethig, R. *Dielectric and Electronic Properties of Biological Materials*; Wiley: Chichester, 1979.
(28) Rees, D. C. *J. Mol. Biol.* **1980**, *141*, 323.
(29) Russell, A. J.; Fersht, A. R. *Nature*, **1987**, *328*, 496.
(30) Russell, A. J.; Thomas, P. G.; Fersht, A. R. *J. Mol. Biol.* **1987**, *193*, 803.
(31) Wipff, G.; Blaney, J.; Weiner, P.; Dearing, A.; Kollman, P. A. *J. Am. Chem. Soc.* **1983**, *105*, 997.

We examined the importance of electrostatic interactions between active site residues of triosephosphate isomerase and portions of the substrate dihydroxyacetone phosphate. Our results indicate that the charge interactions examined contribute equally to binding in the wild-type and Asp 165 mutant enzymes. This is consistent with the experimental observation that substrate binding does not change substantially upon replacement of Glu 165 by Asp. Furthermore, our results suggest that less effective interactions between Lys 13 and the non-phosphate portion of DHAP in the mutant transition state for enolization may, at least partially, explain the observed drop in catalytic activity upon mutation of Glu 165 to Asp. Other explanations for the observed drop in k_{cat} have been proposed, and more simulations and the X-ray structure of the mutant are required to differentiate between the possibilities.

Acknowledgment. We are grateful for research support from NIH (GM-29072) and for essential graphical visualization of our results provided by the UCSF Computer Graphics Lab (RR-1081, R. Langridge, Director). The purchase of the FPS array processor was made possible through grants from the NIH (RR-02441) and NSF (DMB-84-13762), and their support for this is much appreciated. We thank J. F. Bazan for making the figures, R. T. Raines for helpful comments, and U. C. Singh for computational assistance.

Registry No. TIM, 9023-78-3; DHAP, 57-04-5; Glu, 56-86-0; Asp, 56-84-8; Lys, 56-87-1.

(32) Kollman, P. A.; Dearing, A.; Weiner, P. *Biopolymers* **1981**, *20*, 2583.
(33) Singh, U. C.; Pattabiramin, N.; Kollman, P. A. *Proc. Natl. Acad. Sci. U.S.A.* **1986**, *83*, 6402.

ESR Study of 2-Substituted 2-Adamantyl Radicals. Configuration and Long-Range Hyperfine Interaction[1]

Mitsuo Kira,* Mieko Akiyama, Michiko Ichinose, and Hideki Sakurai*

Contribution from the Department of Chemistry, Faculty of Science, Tohoku University, Aoba-ku Sendai 980, Japan. *Received March 31, 1989*

Abstract: Structure and long-range hyperfine interaction in 2-adamantyl, 5,7-dimethyl-2-adamantyl, and the various 2-substituted radicals (substituent = CH_3, CH_2SiMe_3, $OSiMe_3$, $SSiMe_3$, CH_2GeMe_3, etc.) were studied by ESR. The origin of the long-range hyperfine interaction is discussed on the basis of the comparison between experimental and theoretical hfs values. The pyramidality of the radical center introduced by a proper substituent at the 2-position of 2-adamantyl radicals has been found to exert significant influence to the long-range interaction. The analyses of hfs values for persistent 2-bis(trimethylsilyl)methyl-2-adamantyl radical and the 5,7-dimethyl derivative were made by the assistance of the ENDOR spectrum. The very small hfs values observed for the bis(trimethylsilyl)methyl methine protons not only show almost perpendicular arrangement of the C_α–H_β bond to the singly occupied pπ orbital but also suggest that the constant A in the Heller–McConnell equation would be positive on the basis of the positive temperature dependence.

The electronic and geometric structure of organic radicals has been usually discussed on the basis of the ESR hyperfine splitting (hfs) values. Among them, the hfs values due to the α and β protons are of primary importance since the mechanism of the interactions has been well established theoretically and these hfs values can be related to the empirical expressions such as the McConnell[2] and the Heller–McConnell[3] equations. The hfs values for more remote protons (γ, δ, etc.) have also been known to depend on the radical geometry.[4] Considerable effort has centered

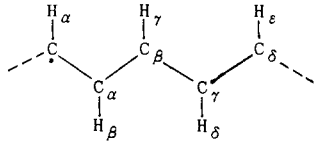

on establishing the reasonable relationship between the long-range proton hfs and the radical structure.[5] Recent experimental[6] and theoretical[7] studies have shown that the long-range hfs values are actually promising as a structural probe for the geometry of the distant region from the radical center.

2-Adamantyl radicals may constitute one of the most suitable models for not only experimental but also theoretical studies of the long-range hyperfine interactions as they possess a rigid hydrocarbon framework with minimum strain. In addition, by introducing a proper substituent at the 2-position of the 2-adamantyl radical, the effect of pyramidality of the radical center on the long-range hfs values would be examined. In spite of a number of ESR studies on 2-adamantyl radicals in adamantane matrix[8] as well as in solution,[9] the hfs parameters had not been determined accurately before we accomplished the present study.[10] Moreover, γ-irradiation of adamantane studied by different groups has produced conflicting results.[4] We now report the first detailed study of the ESR spectra of 2-adamantyl and 2-substituted 2-adamantyl radicals and discuss the long-range hyperfine interaction in this system. It should be stressed that the main difficulty in assigning the hfs values of 2-adamantyl radical has been overcome by comparing the ESR parameters with those of 5,7-

(1) Chemistry of Organosilicon Compounds. 262.
(2) McConnell, H. M. *J. Chem. Phys.* **1956**, *24*, 632, 764.
(3) Heller, C.; McConnell, H. M. *J. Chem. Phys.* **1960**, *32*, 1535.
(4) King, F. W. *Chem. Rev.* **1976**, *76*, 157.
(5) (a) Underwood, G. R.; Vogel, V. L.; Iorio, J. *Mol. Phys.* **1972**, *25*, 1093. (b) Sullivan, P. D.; Wright, W. L. *J. Magn. Reson.* **1974**, *13*, 232. (c) Barfield, M. *J. Phys. Chem.* **1970**, *74*, 621.
(6) (a) Ingold, K. U.; Walton, J. C. *J. Am. Chem. Soc.* **1982**, *104*, 616. (b) Ingold, K. U.; Nonhebel, D. C.; Walton, J. C. *J. Phys. Chem.* **1986**, *90*, 2859.
(7) (a) Ellinger, Y.; Subra, R.; Levy, B.; Millie, P.; Berthier, G. *J. Chem. Phys.* **1975**, *62*, 10. (b) Ellinger, Y.; Rassat, A.; Subra, R.; Berthier, G. *J. Am. Chem. Soc.* **1973**, *95*, 2372.
(8) (a) Gee, D. R.; Fabes, L.; Wan, J. K. S. *Chem. Phys. Lett.* **1970**, *7*, 311. (b) Ferrell, J. R.; Holdren, G. R., Jr.; Lloyd, R. V.; Wood, D. E. *Ibid.* **1971**, *9*, 343. (c) Lloyd, R. V.; Rogers, M. T. *Ibid.* **1972**, *17*, 428. (d) Hyfantis, G. J.; Ling, A. C. *Can. J. Chem.* **1974**, *52*, 1206. (e) Migita, C. T.; Iwaizumi, M. *Chem. Phys. Lett.* **1980**, *71*, 322. (f) Lloyd, R. V.; DiGregorio, S.; DiMauro, L.; Wood, D. E. *J. Phys. Chem.* **1980**, *84*, 2891.
(9) (a) Scaiano, J. C.; Ingold, K. U. *J. Am. Chem. Soc.* **1976**, *98*, 4727. (b) Conlin, R. T.; Miller, R. D.; Michl, J. *Ibid.* **1979**, *101*, 7637. (c) Ieli, S. *Chim. Acta Turc.* **1979**, *7*, 261. (d) Waltman, R. J.; Ling, A. C.; Bargon, J. *J. Phys. Chem.* **1982**, *86*, 325.
(10) For preliminary communication, see: Kira, M.; Watanabe, M.; Ichinose, M.; Sakurai, H. *J. Am. Chem. Soc.* **1982**, *104*, 3762.

0002-7863/89/1511-8256$01.50/0